Reduction of the mutual coupling between implanted microstrip antennas on a cylindrical biocompatible metallic ground plane

Jie Huang
Department of Electronics and Telecommunications
Politecnico di Torino - Italy
+86 15236293747
janemeloo1314@gmail.com

Ildiko Peter
Department of Applied Science and Technology
Politecnico di Torino - Italy
+39 011 090 4670
ildiko.peter@polito.it

Ladislau Matekovits
Department of Electronics and Telecommunications
Politecnico di Torino - Italy
+39 011 090 4119
ladislau.matekovits@polito.it

ABSTRACT
The effect of mutual coupling between two antennas within a human body model is studied. The multilayer model includes highly lossy materials in which biocompatible metal implant is inserted, that in the present study serves as a ground plane of the conformal radiators. The effect of the mutual coupling between two antennas sharing the same ground plane is numerically studied and quantified. For its reduction a grounded microstrip line configuration is proposed, that can be easily inserted in the considered geometry. Its presence increases the directivity of the 2-element conformal array and reduces the level of the sidelobes.

CCS Concepts
• Hardware → Printed circuit boards → Electromagnetic interference and compatibility • Hardware →Communication hardware, interfaces and storage → Signal processing systems → Beamforming.

Keywords
Implanted antenna, mutual coupling reduction, In-body wireless electronic

1. INTRODUCTION
Medical telemetry - also called biotelemetry- involves the application of telemetry in medicine and other healthcare. It allows remotely monitoring various vital signals of ambulatory patients and it is exploited more and more in the today healthcare system. If adequately implemented, i.e., allowing real-time transmission of biological signals from the body - as the human temperature, blood pressure and to monitor of cardiac beat in sickrooms, etc., - in a plausible way to a far located medical center, it is possible to distantly monitor patient and for example to send medical team just if necessary. The use of such technologies can strongly reduce hospitalization time, and consequently associated costs, without affecting the efficiency of the service. On the other hand, having the possibility to continuously collect the biological data, algorithms to predict the evolution of the medical condition of the patients can also be developed, which again can reflect in a higher quality of the service, for example by considering recovery only when in fact necessary.

In some cases, on-body sensors can collect the signal of interest, but in other cases, the information has to be obtained from inside the body. In this case, the collected information should be transmitted outward from inside the body. Implanted antennas are the basic elements of any of such system, where communication between an implanted device in the human body with the outside receivers is required.

The location of the implanted antennas depends on the given application. Some of them, e.g., for a wireless RF powered brain machine interface applications are located in brain [1], [2]. In [1] it is shown that the position of the implanted antenna and electrical properties of insulating layer will also affect the RF power reception and the properties of the tissues surrounding the implanted antenna can influence the electrical characteristics of the antennas. In [2] a planar spiral antenna (PSA) is designed in the brain to detect the existence of tumor. In the presence of tumor, the resonant frequency of the PSA is larger than for healthy tissues. Other antennas are implanted in human arms. In [3], an implanted cavity slot antenna with H-shape slot is proposed and characterized. Few examples of antennas on the bone are in [4], [5]. In [4] an implanted antenna located between the two parts of a broken femur is considered. It consists of a conformal slot array that is part of a wireless battery system. In [5], the reason of using implanted antennas in bone rather than in the muscle and skin is discussed: a comparison between bone implanted antenna and muscle implanted antenna is presented.

Radiation performances of antennas can be increased, for example, by considering an array of radiators. This solution also presents some drawbacks, as the larger dimension of the antenna, and the effect of the mutual coupling between the radiators, that can, in turn, reduce the gain or increase the level of sidelobes. In the literature, different ways to reduce the effect of the mutual coupling have been proposed. In [6], parasitic tape on microstrip patch elements is experimented. This mechanism of mutual coupling reduction has been studied by observing the field distribution in the presence of the tape, and compare it with the initial case when the tape is not present. In [7], a solution consisting of the use of one pair of slit between two walls of a printed circuit board in air is studied aiming to improve the isolation of a pair of closely packed antenna elements. In [8], a suspended line that links 2 planar inverted-F antennas (PIFAs) is used to compensate the coupling.

BODYNETS 2016, December 15-16, Turin, Italy

DOI 10.4108/eai.15-12-2016.2267653

By this way, an opposite coupling can be introduced that if properly designed will offset the unwanted interaction and in turn can increase the antenna efficiency. Similar solution is proposed in [9], where a connection between two ports is considered. Such a solution is convenient and easy to be implemented by suitably designing the dimension of the connection. However, the reduction of the coupling i.e., S_{21} parameter, is put side-by side by a shift of the resonant frequency. Another class of solutions for reducing the mutual coupling between radiators consist of using Electromagnetic Band-gap (EBG) structures. In [10], a periodic structure on a conformal ground plane, which exhibits EBG in the interested band, is used. In [11], a defected ground structure (DGS) with two H-shaped slots between the antennas are used which are placed very closely each to other (distance less than 0.3λ). With this structure, the mutual coupling reduces up to 50 dB without significant influence on the radiation pattern. In [12], a comparison between an EBG structure and DGS structure is performed. However, the study of the mutual coupling for implanted antennas is at the early stage, and at the best of the authors' knowledge, only few examples are reported in the literature.

Bearing in mind the classes of the implanted antennas, where space and material constrains are to be strongly considered in this paper, the reduction of the mutual coupling in the case of an implanted 2-element antenna array is investigated. The radiators are placed on a metallic cylinder (the implant) embedded in a polymer dielectric that acts as a substrate between the ground plane and radiators, all of them being conformal. For the reduction of the coupling, a narrow, grounded microstrip line is inserted between the antennas. Quantification of the coupling with and without the proposed shield is performed, and the amount of the reduction of the coupling is studied for different positions of the two radiators. In each cases, the grounded line is positioned midway between the radiators. The solution does not require any additional space, since the grounded line is located in the already available space halfway between the antennas.

2. THE BODY MODEL

In this paper a cylindrical body model is considered, that has dimensions similar to an adult leg. The different tissues are modeled as concentric cylinders characterized with different thicknesses and material parameters. A CAD model of the geometry under investigation is presented in Fig. 1.

The material parameters, i.e., relative dielectric constant and conductivity (S/m) are reported in Tab. 1. In all cases the magnetic properties of the different tissues and dielectric have been neglected, i.e. a relative magnetic permeability equal to 1 has been considered.

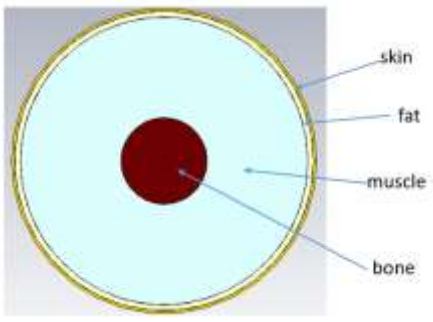

Figure 1. Cross section of the considered geometry.

Table. 1: Characteristics of the different tissues at f=2.45 GHz and metal (implant and antenna)

	muscle	fat	skin	PDMS layer	Bone (Titan)
Epsilon (relative)	57.1	5.6	46.7	2.667	Lossy metal
El.Cond. (S/m)	0.79	0.04	0.69	0.034	1e7

In the considered model, the central part of the geometry in Fig. 1, i.e., the bone, is replaced by an implant of the same dimensions made up by a biocompatible metal chosen between the most commonly used as stainless steels (maybe the cheapest solution), titanium and its alloys, cobalt and its modified compositions, etc.. However, because of their encouraging mechanical properties, high corrosion resistance and thanks to their exceptional biocompatibility Ti and its alloys are the foremost materials used in the orthopedic field. In particular, Ti–6Al–4V is used in a multiplicity of stress-bearing orthopedic applications, but some investigations [13, 14] have demonstrated that the release of Al and V ions can progressively determine well-being problems. Because of this, recently the attention is focalizing on the study of Al, V-free metallic alloys: starting from a basic Ti alloys composition and replacing the risky elements by Nb, Ta, Mo, Zr or a mixture of them, such release can be significantly reduced or even eliminated. Zr belongs to the same group as Ti and it shows an allotropic transformation similar to that of Ti. Both Ta and Nb are non-toxic elements and reveal very alike physical and chemical properties. Because of their good biocompatibility and high corrosion resistance, these metals have been employed as constituent elements of Ti alloys even for the applications under investigation in the present paper. Ta exhibits excellent chemical stability and good biocompatibility similar to that of Ti. In particular, porous Ta has been developed for bone in-growth applications, for example hip and knee arthroplasty. Besides, introduction of Ta in Ti-Ni shape memory alloy leads to a reduced happening of artifacts: the blood compatibility of Ta was supposed to be higher, compared to other metals [15-22]. These are just some aspects why Ti and its alloys are used for the considered investigation.

Such a large extension metallic part is used as ground plane for a conformal rectangular microstrip antenna as reported in the model in Fig. 2.

The antenna is separated from the metallic cylinder by a conformal substrate made up of Polydimethylsiloxane (PDMS). In the considered model, a second layer of PDMS is also present that acts

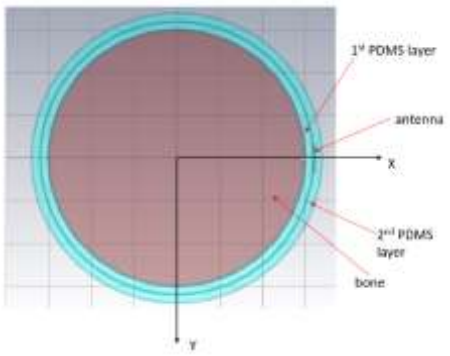

Figure 2. Position of the conformal antenna and PDMS substrate and superstrate with respect to the implant "bone".

as superstrate. In the numerical modelling, the thicknesses of the two PDMS layers, are considered equal. The other leading dimensions are reported in Tab. 2

Table. 2: The parameters of the model

Parameter	Description	Value (mm)
r_{bone}	The radius of the bone	30
l_{str}	The overall length of the structure	100
l_{PDMS}	The length of the PDMS layer	66
th_{PDMS}	The thickness of the PDMS layer	2
th_{muscle}	The thickness of the muscle	70
th_{met}	The thickness of the metal	0.5
th_{fat}	The thickness of the fat	4
th_{skin}	The thickness of the skin	2

3. DESIGN A SINGLE ANTENNA

In the first step of the analysis, a single antenna element has been designed. It is a rectangular microstrip patch antenna of length l_{ant} and width w_{ant}, fed by a probe on its symmetry axis, and at a distance l_z from one of the edges. The three aforementioned parameters have been used in an optimization process to minimize the reflection coefficient with respect to standard 50 Ω at the center of the 2.4 - 2.5 GHz Industrial, Scientific and Medical (ISM) radio band, i.e. at 2.45 GHz. The optimization process was necessary, since considering the body environment, no analytic formulas for the design are available. After the optimization by Genetic Algorithm, the dimensions of the antenna result to be l_{ant}=32 mm, w_{ant}=7 mm and l_z=0 mm, respectively. The corresponding reflection coefficient is reported in Fig. 3.

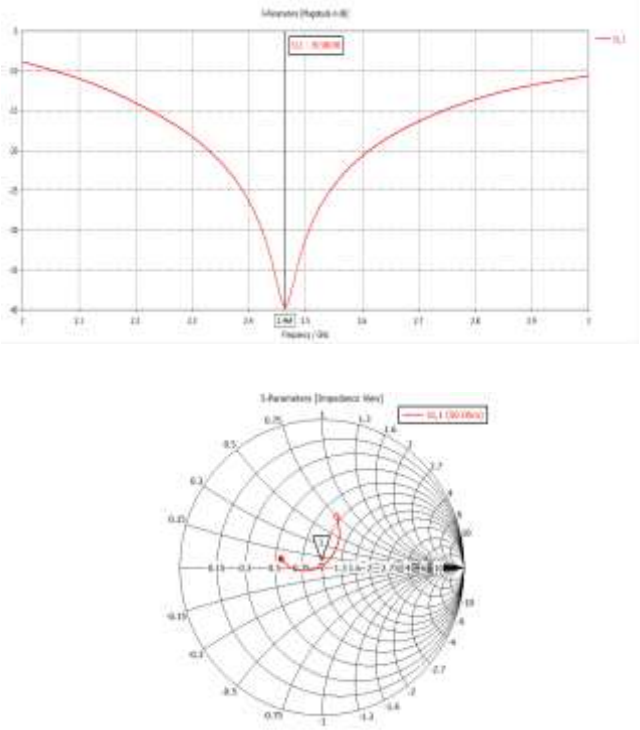

Figure 3. Impedance matching of the optimized antenna.

The resulting geometry exhibits a good matching at 2.464 GHz, which is close the center of the considered band, and a good bandwidth (also due to the losses considered in the simulation).

4. QUANTIFYING THE MUTUAL COUPLING

As mentioned above, our interest is the quantification of the coupling between two antennas. The corresponding scenario is presented in Fig. 4. Two identical antennas have been considered. The first one is considered in a fix position, and the second one is moved around the implant by an angle alpha.

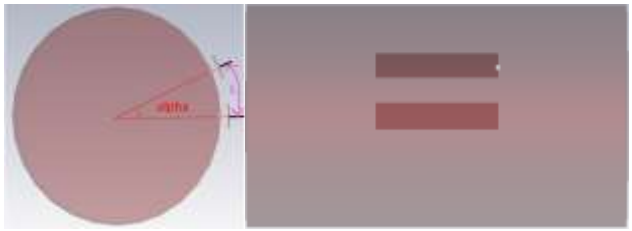

Figure 4. Model of the two parallel antennas around the cylindrical implant: front view (left), side view (right).

The complex scattering matrix has been computed and the mutual impedance Z_{21} evaluated for different rotation angles alpha, in the interval from 25° to 180° with a step of 5°. The corresponding results are reported in Fig. 5.

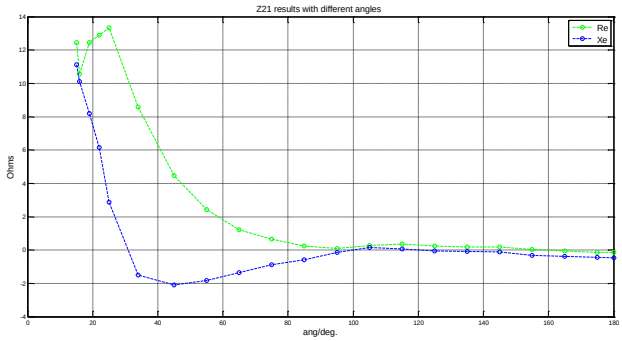

Figure 5. Real and imaginary part of the mutual impedance between the two dipoles for different rotation angles.

From the data in Fig. 5 it results that the coupling has an oscillatory behavior and presents a strong reduction while the distance between the antennas increases, similar to what happens for the planar case [23].

However, since the active input impedance Z_{inp} of the single element is influenced by the self-impedance of the two elements Z_{11} and Z_{22}, respectively, and by the mutual coupling Z_m according to

$$Z_{inp} = Z_{11} - \frac{Z_m^2}{Z_{22}}$$

for small angles the large coupling can have a significant effect. In order to reduce this influence, in the following section a solution for the reduction of the mutual coupling is proposed and analyzed.

5. REDUCTION OF THE MUTUAL COUPLING

A common practice to reduce mutual coupling between parallel lines (as our geometry can be approximated) is to introduce a grounded line between the two antennas. The corresponding model is shown in Fig. 6.

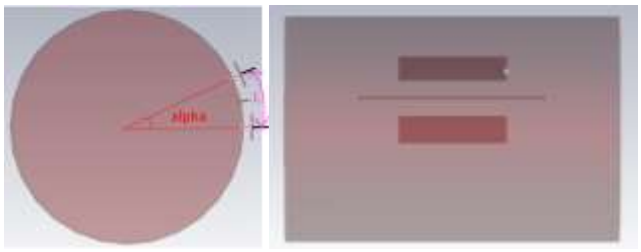

Figure 6. Model of the two parallel antennas around the cylindrical implant separated by a grounded narrow microstrip line: front view (left), side view (right).

The material of the line is the same as of the implant and antennas. Its width has been chosen to be equal to 0.4 mm. As concern its length, it has been chosen in such a way to avoid resonance; the value of 55 mm has been used in the following simulations performed in the angular interval of 25º to 90º. The two ends of the line are connected to the implant by two metallic cylinders. The values of the scattering matrix entries for the two analyzed cases, i.e. no line, and presence of the grounded line, respectively, are reported in Fig. 7.

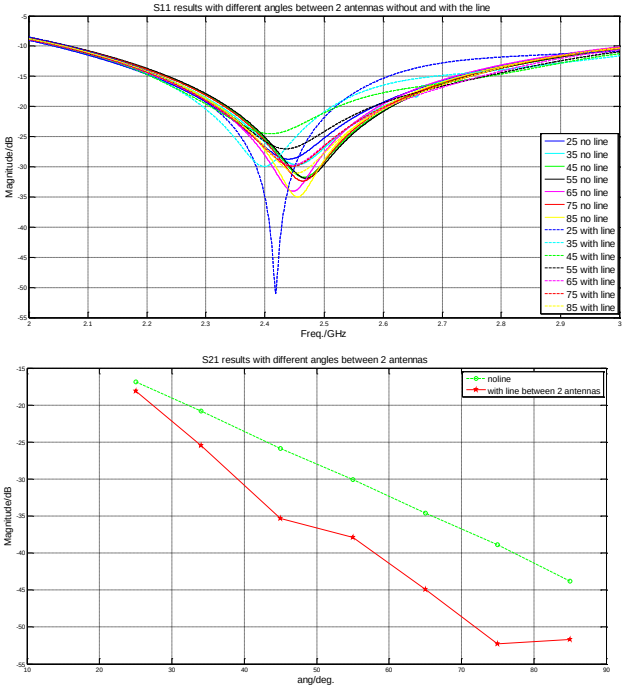

Figure 7. Reflection (top) for the initial (solid line) and proposed scheme (dotted line) and transmission coefficient (bottom) for the initial ("circle") and proposed scheme ("star").

As it can be observed, the presence of the grounded line between the antennas reduces the mutual coupling between them while their resonance frequencies are only marginally affected. It is significant that at 75º, the coupling is reaching the maximum reduction, and at 25º, the reduction is minimum.

In the following, the effects of the proposed scheme on the radiation performances is analyzed for the separation angles when the reduction of the coupling is minimum, namely for 25º. Moreover a broadside configuration has been considered, i.e., where the phase difference between the feeding signal of the two antennas is equal to zero. As results from the plots in Fig. 8, presence of the line reflects in a higher directivity that increases from 6.195 dBi to 6.59 dBi, i.e., about 0.4 dBi increment, and lower sidelobes, as expected. The scan of approximatively 12º is due to the fixed position of one of the antennas, while the second one is positioned at 25º, as mentioned above.

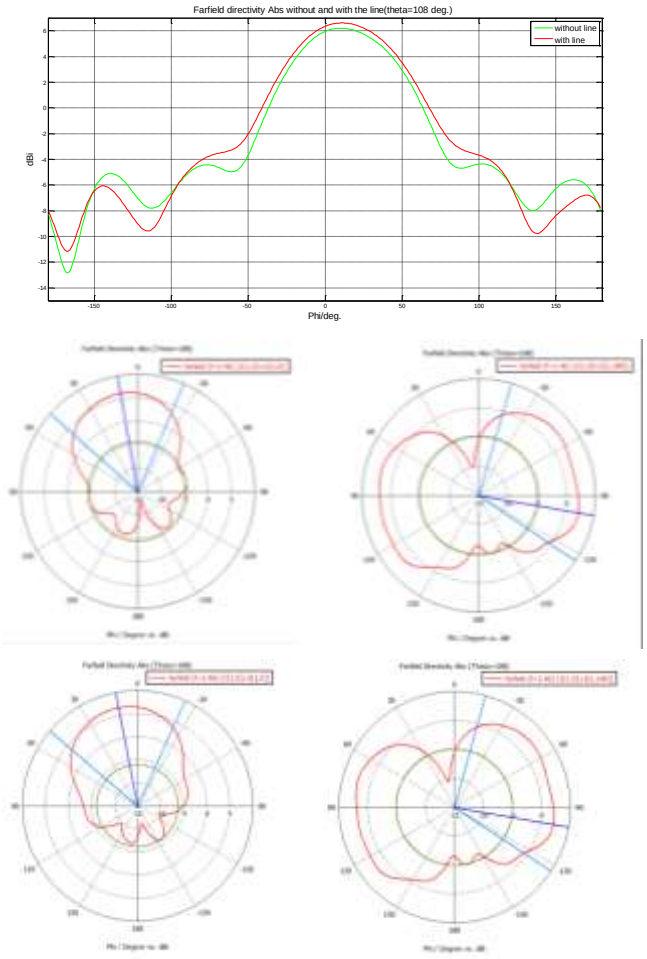

Figure 8. Directivity (top) and radiation patterns of the 2-element array for alpha=25º: initial case (middle) and with the proposed solution (bottom).

6. CONCLUSIONS

A simple method to reduce the coupling between two implanted microstrip antennas has been proposed. It consists of the insertion of a grounded, non-resonant narrow microstrip line halfway between the radiators. The effect of the coupling reduction has been quantified, and it was numerically verified that the reduced coupling manifests in a higher directivity and lower sidelobes of the antenna, as expected.

7. REFERENCES

[1] Zhao, Y., Rennaker, R., Hutchens, C., Ibrahim, T. S., Simulation of Implantable Miniaturized Antenna for Brain Machine Interface Applications.

[2] Shokry M.A., Allam A.M.M.A., Implanted Antenna in Brain ,*IEEE Antennas and Propagation Conference (LAPC), 2013 Loughborough*, DOI= http://dx.doi.org/10.1109/LAPC.2013.6711977

[3] Xia W., Saito K., Takahashi M., Ito K., "Performances of an Implanted Cavity Slot Antenna Embedded in the Human Arm", *IEEE Transactions on Antennas and Propagation*, Vol.57, No.4, April 2009. DOI= http://dx.doi.org/10.1109/TAP.2009.2014579

[4] Zakavi P., Karmakar N. C., Griggs I., Wireless Orthopedic Pin for Bone Healing and Growth: Antenna Development, *IEEE Transactions on Antennas and Propagations*, vol. 58, no. 12, pp. 4069 - 4074, December 2010. DOI= http://dx.doi.org/10.1109/TAP.2010.2078459

[5] Alrawashdeh R., Huang Y., Sajak A.A.B., A Flexible Loop Antenna for Biomedical Bone Implants, *8th European Conference on Antennas and Propagation (EUCAP)*, 2014. DOI= http://dx.doi.org/10.1109/EuCAP.2014.6901898

[6] Wang H., Fang D., Ge P., Mutual coupling reduction between two conformal microstrip patch antennas, *Proc. of 5th Asia-Pacific Conference on Environmental Electromagnetics, 2009. (CEEM 2009)*, 2009, pp. 176 –179. DOI= http://dx.doi.org/10.1109/CEEM.2009.5304778

[7] Neyestanak A. A. L., Jolani F., Dadgarpour M., Mutual coupling reduction between two microstrip patch antennas, *in Proc. of Electr. Comput. Eng.*, 2008, pp. 739–742. DOI= http://dx.doi.org/10.1109/CCECE.2008.4564633

[8] Diallo A., Luxey C., Thuc P. L., Staraj R., Kossiavas G., Study and reduction of the mutual coupling between two mobile phone PIFAs operating in the DCS1800 and UMTS bands, *IEEE Trans. Antennas Propag.*, vol. 54, no. 11, pp. 3063–3074, Nov. 2006. DOI= http://dx.doi.org/10.1109/APS.2008.4620064

[9] Ezzat M., Lee C.S., A simple optimization technique for reducing mutual coupling between two coupled antennas, *2015 IEEE International Symposium on Antennas and Propagation & USNC/URSI National Radio Science Meeting*, 2008, DOI= http://dx.doi.org/10.1109/CCECE.2008.4564633

[10] Kawakami, Y., Hori, T., Fujimoto, M., Yamaguchi, R., Cho, K., Mutual coupling reduction effects of EBG structure located on cylinder surface. *Antennas and Propagation Society International Symposium (APSURSI)*, 2010 IEEE, Page(s): 1 - 4. DOI= http://dx.doi.org/10.1109/APS.2010.5561160

[11] Acharjee J., Mandal K., Mandal S.K., Sarkar P.P., Mutual coupling reduction between microstrip patch antennas by using a string of H-shaped DGS, *2016 International Conference on Microelectronics, Computing and Communications (MicroCom)*, 23-25 Jan. 2016, DOI= http://dx.doi.org/10.1109/MicroCom.2016.7522477

[12] Mahmoud A. Abdalla, Ahmed M. Abdelreheem, Mohamed H. Abdegellel, Ali M. Ali, Surface Wave and Mutual Coupling Reduction Between Two Element Array MIMO Antenna, *Antennas and Propagation Society International Symposium (APSURSI), 2013 IEEE*, DOI= http://dx.doi.org/10.1109/APS.2013.6710750

[13] Cvijovic Alagic I., Gubeljak N, Rakin M, Cvijovic Z, Geric K., Microstructural morphology effects on fracture resistance and crack tip strain distribution in Ti–6Al–4V alloy for orthopedic implants. *Materials Design* 53 (2014) 870–80. DOI= http://dx.doi.org/10.1016/j.matdes.2013.07.097

[14] Wen M., Wen C., Hodgson P., Li Y., Fabrication of Ti–Nb–Ag alloy via powder metallurgy for biomedical applications, *Materials Design* 56 (2014) 629–634. DOI= http://dx.doi.org/10.1016/j.matdes.2013.11.066

[15] Zardiackas LD, Mitchell DW, Disegi JA., In: Brown SA, Lemons JE, editors. Medical applications of titanium and its alloys: the material and biological issues. West Conshohocken (PA): *ASTM International* (1996) 60‑75.

[16] Kondo R, Nomura N, Suyalatu, Tsutsumi Y, Doi H, Hanawa T., Microstructure and mechanical properties of as-cast Zr–Nb alloys, *Acta Biomaterials* 7 (2011) 4278–4284. DOI= http://dx.doi.org/10.1016/j.actbio.2011.07.020

[16] Suyalatu, Kondo R, Tsutsumi Y, Doi H, Nomura N, Hanawa T., Effects of phase constitution on magnetic susceptibility and mechanical properties of Zr-rich Zr–Mo alloys, *Acta Biomaterial* 7 (2011) 4259–4266. DOI= http://dx.doi.org/10.1016/j.actbio.2011.07.005

[17] Ho WF, Chen WK, Wu SC, Hsu HC., Structure, mechanical properties and grindability of dental Ti‑Zr alloys, *Journal of Material Science ‑ Matererials Medicine* 19 (2008) 3179‑8316. DOI= https://dx.doi.org/10.1007/s10856-008-3454-x

[19] Takahashi M., Kikuchi M., Okuno O., Grindability of dental cast Ti‑Zr alloys, *Materials Transaction* 50 (2009) 859‑863. DOI= http://dx.doi.org/10.2320/matertrans.MRA2008403

[20] I. Peter, M. Rosso, Study of Ti-enriched CoCrMo alloy for dental application, *IEEE Access*, Vol.3 (2015) 73-80. DOI= http://dx.doi.org/10.1109/ACCESS.2015.2398312

[21] Ho WF, Ju CP, Chern Lin JH., Structure and properties of cast binary Ti‑Mo alloys, *Biomaterials* 20 (1999) 2115‑2122. DOI= http://dx.doi.org/10.1016/S0142-9612(99)00114-3

[22] Ho WF., A comparison of tensile properties and corrosion behavior of cast Ti‑7.5Mo with c.p. Ti, Ti‑15Mo and Ti‑6Al‑4V alloys, *J Alloys Compounds* 464 (2008) 580‑583. DOI= http://dx.doi.org/10.1016/j.jallcom.2007.10.054

[23] John D. Kraus, Antennas, New York: McGraw-Hill, 1950.